EIS on plasma-polymerised coatings used as pre-treatment for aluminium alloys

L. Domingues [a], C. Oliveira [a], J.C.S. Fernandes [a,*], M.G.S. Ferreira [a,b]

[a] *Department of Chemical Engineering, Instituto Superior Técnico, 1049-001 Lisboa, Portugal*
[b] *Department of Ceramics and Glass Engineering, Universidade de Aveiro, 3810-193 Aveiro, Portugal*

Abstract

Plasma coatings from hexamethyldisiloxane (HMDSO) have proven to be effective primer coatings for adhesion promotion to aluminium but the corrosion properties of these coatings have not been thoroughly assessed. In the present work, electrochemical impedance spectroscopy (EIS) was used to evaluate the corrosion behaviour of Alclad AA2024-T3 covered with a polymer film prepared by plasma polymerisation, using HMDSO as monomer. The present results indicate that, although the polymer film was mainly intended to provide a strong coupling between the metal substrate and the organic coating, the film in itself confers protection against corrosion. Equivalent circuits are proposed for the immersion behaviour of uncoated and plasma-coated material, allowing the determination of the parameters relative to natural aluminium oxide, coating layer and pitting. An estimation of the water uptake during the immersion time from the values obtained for the coating capacitance was carried out. The evaluation of the corrosion performance of these plasma-coated materials by means of their water uptake behaviour may be useful, as the water volume fraction seems to be much more sensitive to the changes in the system due to delamination than the values obtained from the fitting of EIS data to an equivalent circuit. © 2002 Elsevier Science Ltd. All rights reserved.

Keywords: Plasma polymerisation; Aluminium alloy; Corrosion; Water uptake

1. Introduction

The use of pre-treatments on aluminium alloys prior to painting or adhesive bonding is an essential technology in many industrial sectors (e.g. aerospace industry). However, the pre-treatments used on the substrates, which are vital to ensure reliable long-term performance, often comprise a range of environmentally objectionable chemicals, such as solvents and chromates, some of which are carcinogenic.

The plasma deposition of thin coatings on aluminium, which exhibit strong interfacial bonding, could be an alternative to the traditional chromate-based treatments. It is envisaged that plasma cleaning, etching and deposition could be carried out in a single plasma reactor, providing a complete preparation cycle before painting and avoiding the use, handling and disposal of hazardous materials [1–4].

Plasma coatings from hexamethyldisiloxane (HMDSO) and add-gases such as O_2 have proven to be effective primer coatings for adhesion promotion to aluminium [5] but the corrosion properties of these coatings have not been thoroughly assessed. In the present work, electrochemical impedance spectroscopy (EIS) was used to evaluate the corrosion behaviour of Alclad AA2024-T3 covered with a polymer film prepared by plasma polymerisation, using HMDSO as monomer. This work was included in a wider project, whose main objective was the evaluation of the adhesion properties of the plasma-polymerised coatings prepared under different experimental conditions, and was carried out in order to check whether the coating has a deleterious effect on the environmental resistance of the substrate material [6]. The present results indicate that, although the polymer film was mainly intended to provide a strong coupling between the metal substrate

---
* Corresponding author. Tel.: +351-21-841-7964; fax: +351-21-840-4589.
E-mail address: jfern@ist.utl.pt (J.C.S. Fernandes).

and the organic coating, the film in itself confers protection against corrosion.

The EIS spectra obtained for uncoated Alclad AA2024-T3 in 0.5 M NaCl solutions are presented in the first part of the paper. An equivalent circuit is proposed and the results of the fitting of spectra for different immersion times are discussed.

In the second part, the same procedure is followed for the results obtained on plasma-coated Alclad AA2024-T3. A simple equivalent circuit, similar to the one used for organic paint systems [7,8], is proposed to describe the plasma polymer coating (Fig. 1). Here, the capacitance of the intact coating is represented by C_c, its value being much smaller than a typical double layer capacitance. Ion conducting paths that develop in the coating due to the presence of pores or defects (corresponding to an area fraction of θ) are represented by the resistor R'_Ω in series with the parallel RC contribution of the natural oxide layer on the top of which the coating was applied. The solution resistance R_Ω corresponds to the ohmic drop across the electrolyte.

The third part of the paper involves the analysis of the film capacitance, C_c, which is normally related to the thickness l of the coating layer on the specimen surface by the following equation:

$$C_c = \frac{\varepsilon \varepsilon_0 A}{l}$$

where ε is the dielectric constant of the film (typically 4–8 for organic coatings), ε_0 the electric permittivity of free space ($\varepsilon_0 = 8.854 \times 10^{-12}$ F/m) and A is the true specimen area of the electrode.

After immersion, an increase in the film capacitance can be attributed to water uptake. The water volume fraction ϕ may be estimated from the capacitance of the coating, according to the equation proposed by Brasher and Kingsbury [9]:

$$\phi = \frac{\log(C_t/C_0)}{\log \varepsilon_w}$$

where ε_w is the dielectric constant of water ($\varepsilon_w = 80$), whereas C_t and C_0 represent the capacitance of the
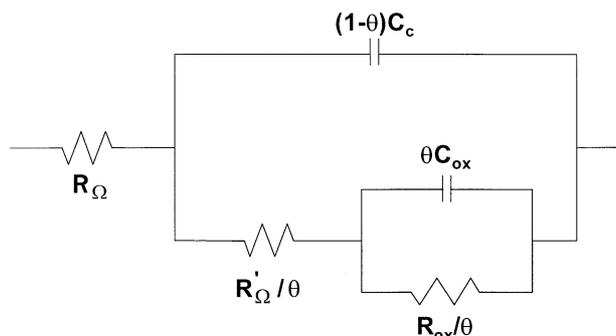
coating after a time t of immersion and at time $t = 0$ (i.e. the dry film capacitance), respectively. The value of the capacitance C_t is normally obtained from impedance measurements at high frequencies, whereas the value of C_0 is extrapolated from the values of capacitance determined from the initial stages of immersion.

Most coatings degrade with time, resulting in a more complex behaviour that is no longer represented by a simple circuit as the one shown in Fig. 1. Normally, water penetrates into the coating and forms a new liquid/metal interface under the coating, where corrosion is likely to occur. In the present study, corrosion failure normally occurs in the form of pitting on defective zones of the coating.

2. Experimental

2.1. Deposition procedure

The plasma polymerisation process was carried out in a 21 litre stainless steel vacuum chamber plasma reactor (Fig. 2), the operational conditions having been described elsewhere [6,10].

The deposition substrate was an aluminium alloy, 2024-T3 Alclad and, prior to plasma deposition, all the samples were wiped by tissues with C_3H_6O. Samples were then placed on the powered electrode.

The plasma processing consisted of two stages: pretreatment and deposition. During the first stage, the Al samples were cleaned in Ar plasma for 5–15 min at 80 mtorr discharge pressure with a -700 V self-bias on the powered electrode. The radio-frequency (RF) generator power was 185 W.

The gas mixture used for coating deposition was prepared by introduction of the add-gas into the chamber (O_2 at a flow of 30 sccm) up to a pressure of 30 mtorr. Then HMDSO vapour was added with its partial pressure being regulated by a metering valve in
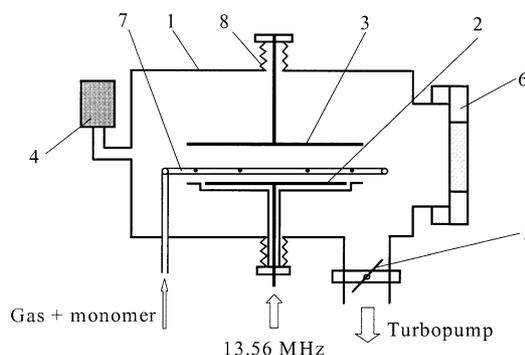

Fig. 2. Diagram of the plasma discharge chamber, where: 1, vacuum chamber; 2, powered electrode; 3, grounded electrode; 4, capacitive pressure gauge (baratron); 5, butterfly valve; 6, vacuum door with viewport; 7, gas shower ring; 8, bellows translational stage.

Fig. 1. Equivalent circuit for a plasma polymer coating.

the monomer line. The gas mixture total pressure was in the range 31–35 mtorr.

The deposition process was conducted typically at a RF power of 11 W with the self-bias voltage in the range −190 to −150 V. Some experiments were conducted at higher power (65 W) leading to self-bias voltages of −500 V. The HMDSO monomer flow (1.3 sccm) was controlled through its partial pressure by regulating the metering valve on the monomer line. The deposition step was carried out until a coating of 200 nm had been deposited on the sample substrate. The time required for this varied from 5 to 20 min, depending on the partial pressure of HMDSO and the RF power. The coating thickness was measured in situ by optical ellipsometry, which is not described in this publication.

2.2. Electrochemical impedance spectroscopy tests

EIS measurements were made in 0.5 M NaCl solutions. Untreated Alclad 2024-T3 was also tested. The experimental set-up for these tests comprised a 1250 Frequency Response Analyser and a 1286 Electrochemical Interface (both from Solartron/Schlumberger) controlled by a PC-compatible computer that also performed the data acquisition and processing. The measurements were carried out by applying to the cell a 10 mV (RMS) sine wave with frequencies in the range of 50 kHz–5 mHz (7.13 points per decade). The behaviour of each sample was followed from the moment of immersion up to 60 days, allowing for the detection of the first corrosion spots (pits). A minimum of two samples, prepared under the same conditions, was tested, in order to evaluate the reproducibility of the results.

Fast impedance measurements were carried out for the study of water uptake by the coatings, where only a few points in the high frequency range were obtained. This procedure allows for the acquisition of one spectrum every 3–4 min, which is needed for the extrapolation of the initial coating capacitance.

3. Results and discussion

Impedance spectra obtained for different immersion times in a 0.5 M NaCl solution for untreated Alclad 2024-T3 and for one of the samples of plasma-coated Alclad 2024-T3 are shown in Figs. 3 and 4, respectively.

The above spectra indicate that the impedance values associated with the plasma-coated material are one order of magnitude higher than the observed for the uncoated alloy. Moreover, even after 50 days of immersion, the coated specimens exhibit higher values than the ones observed for the uncoated specimens at the early stages of immersion.
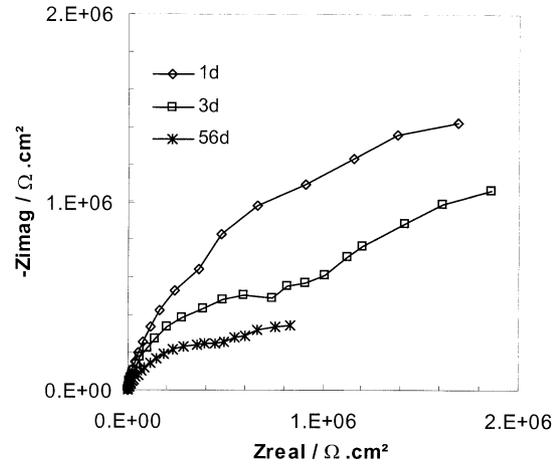
Fig. 3. Impedance plots for untreated Alclad 2024-T3 at different times of immersion in 0.5 M NaCl solution.
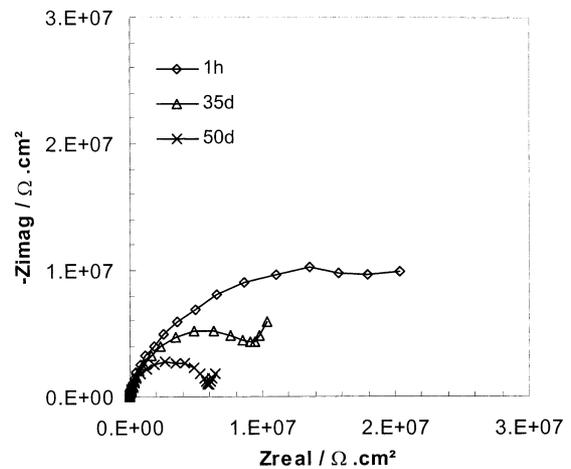
Fig. 4. Impedance plots for plasma-coated Alclad 2024-T3 at different times of immersion in 0.5 M NaCl solution.

The behaviour of the uncoated aluminium alloy may be fitted to the circuit presented in Fig. 5, similar to those normally assigned to localised corrosion and, in
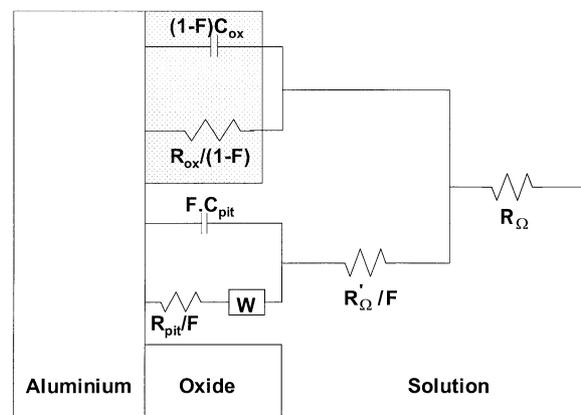
Fig. 5. Equivalent circuit for pitting in aluminium and aluminium alloys.

particular, to pitting corrosion [11–17]. In this circuit, C_{ox} and R_{ox} are, respectively, the capacitance and the resistance of the natural oxide film formed on the aluminium surface, C_{pit} and R_{pit} are the double layer capacitance and the charge transfer resistance corresponding to the area where localised corrosion occurs and W is the Warburg element associated to a pitting process [15–18]. F is the area fraction ($0 \leq F < 1$) affected by pitting and R_{Ω} and R'_{Ω} stand for the ohmic drop in the overall solution and inside the pits.

The results of the fitting for spectra obtained for the uncoated Alclad 2024-T3 alloy at several immersion times generate the plots in Fig. 6. Typical values of 1×10^{-4} or less for χ^2 indicate a good fitting quality.

The above results indicate that, for the uncoated Alclad material, the pitting process begins at the early stages of immersion, i.e. during the first 24 h. This is in contrast with the situation observed by the authors for ultra-pure aluminium (99.999%), where pitting occurs after a longer immersion period [19], but may be explained by the presence of a higher concentration of alloying elements in the cladding aluminium sheet. In fact, the cladding of 2024-T3 consists normally on thin sheets of AA 1230, with 99.30% Al.

It is important to note that the FC_{pit} values for the first 100 h (~4 days) of immersion are very small. Considering for the double layer capacitance C_{pit} a value of 96 μF cm^{-2}, reported by Mansfeld [18] for similar conditions, the results obtained for 24 h immersion ($FC_{pit} = 0.11$ μF cm^{-2}) lead to a value of $F = 0.0012$,

indicating that the pitting process is occurring in a very small area of the specimen. Similar calculations indicate that the area fraction affected by pitting only reaches 1% on the 26th day of immersion.

The variation of $R_{ox}/(1-F)$ was not included in the plot of Fig. 6 because it does not change significantly during the immersion period, showing values in the range of 10–20 MΩ cm^2, which are typical of an aluminium oxide film.

For the plasma-coated Alclad 2024-T3 aluminium alloy, the results of microscopy and XPS measurements indicate the presence of a coating layer with an approximate thickness of 200 nm. In this case, the equivalent circuit used to fit the EIS spectra should include the contribution of the coating that may be considered as similar to a paint layer.

However, the observations of the coated specimens indicate that the plasma-polymer coating shows a porous structure and that there are some defects, leading to localised uncoated zones.

The development of an equivalent circuit corresponding to the presence of the organic layer over a natural oxide covered metal (Fig. 7) should then take into account the presence of a certain area fraction θ of defects in that coating, reaching zones covered with aluminium oxide. The contribution of the organic layer includes a film capacitance C_c and a coating resistance R_c in series with the C_{ox} and R_{ox} relative to the natural aluminium oxide layer, all these elements being weighted by the respective area fraction $(1-\theta)$. The presence of the defects is represented with an additional solution resistance R'_{Ω}/θ in series with the contribution of the natural oxide on the bottom of the defect. In fact, the coating resistance is usually so high ($R_c > 10^8$ Ω cm^2) that the resistor association $R_{ox}/(1-\theta) + R_c/(1-\theta)$ is not detectable in the overall circuit. The series association of the capacitance $(1-\theta)C_{ox}$ and $(1-\theta)C_c$, where C_c is much lower than C_{ox}, also degenerates in just one capacitance, which is approximately equal to the lowest value of C, i.e. to $(1-\theta)C_c$. The equivalent circuit
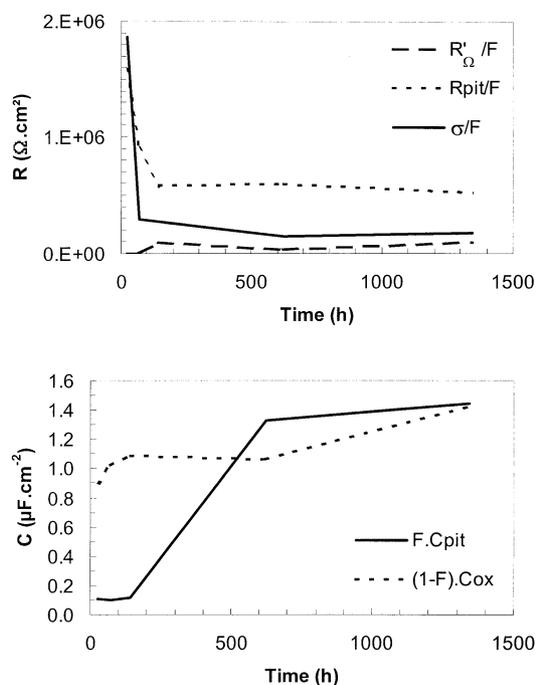

Fig. 6. Evolution of the parameters obtained from the fitting of the spectra measured for uncoated Alclad 2024-T3 at different immersion times in 0.5 M NaCl solution.
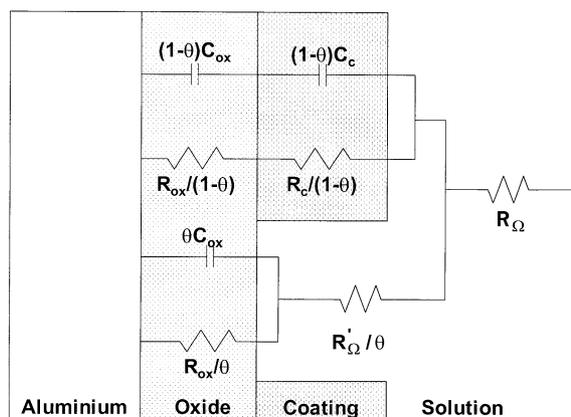

Fig. 7. Equivalent circuit for plasma-coated aluminium alloy.

applicable to the plasma-coated aluminium alloy is then reduced to the form presented in Fig. 1.

The results of the fitting to this equivalent circuit of spectra obtained for the plasma-coated Alclad 2024-T3 alloy at several immersion times generate the plots presented in Fig. 8. Despite the high scattering observed, the results indicate a good fitting up to 700 h of immersion. Up to that moment, R_{ox} distributes over a low slope trend line (gray line in Fig. 8) with values typical of an oxide film. For longer immersion times, the formation of active pits on the aluminium surface is detected and the circuit presented in Fig. 1 is no longer valid. With the onset of pitting corrosion, the results of the fitting of R_{ox} drop to values typical of a charge transfer resistance, whereas C_{ox} rises to very high values normally obtained in the presence of pits if an element such as W is not included. Comparing the results obtained for R_{ox}/θ in Fig. 8 with the ones shown for the uncoated alloy (Fig. 6), it would be expectable to obtain much higher values for the plasma-coated material, as the fraction area of exposed oxide is lower in this case, as $\theta \ll (1-F)$. However, the plasma deposition procedure includes a cleaning/etching pretreatment where it is expected that the natural aluminium oxide should be thinned by sputtering, under the effect of the Ar plasma, so lower values of R_{ox} would be expected. The same applies to C_{ox}, which may increase for a thinner oxide layer, so the θC_{ox} values are consistent with the model.

The analysis of the values obtained for the coating capacitance was carried out in order to obtain an estimate of the water uptake during the immersion time, according to the Brasher and Kingsbury equation presented above, and is presented in Fig. 9.

From a departing value of 4.8×10^{-8} F cm^{-2}, the values of C_c show a first rise up to a plateau of approximately 6.0×10^{-8} F cm^{-2}, indicating a water volume fraction of 4–5%, similar to the figures found by other authors for organic coatings [8,20]. For longer immersion times, a new rise in C_c is detected, being

Fig. 9. Evolution of the coating capacitance and water uptake for plasma-coated Alclad 2024-T3 at different immersion times in 0.5 M NaCl solution (θ was considered as approximately 0).

attributed to delamination of the coating [21], which may be considered as the precursor of the onset of pitting corrosion. The resulting water volume fractions become too high for a water absorption process and may not be considered as real. In fact, the calculation of this parameter is based on the assumption that the system shows a capacitive behaviour, and this is no longer valid in the presence of delamination or pitting corrosion.

In order to have a more detailed information on the water uptake by the plasma coating, fast impedance measurements were carried out, where only a few points, in the high frequency range, were obtained. One of such spectra was recorded every 3–4 min during the 1st day of immersion, this periodicity being reduced for longer immersion times. Comparing the water uptake plots obtained for a 'very good' specimen, i.e. a plasma-coated sample that did not show pitting corrosion up to the 60th day of immersion (Fig. 10, line a), and for a sample that has shown visible pitting spots on the 23rd day of immersion (Fig. 10, line b) a very different pattern is observed. In fact, for the 'very good' specimen a plateau in the water volume fraction of approximately 6% is obtained after 48 h of immersion, and no further
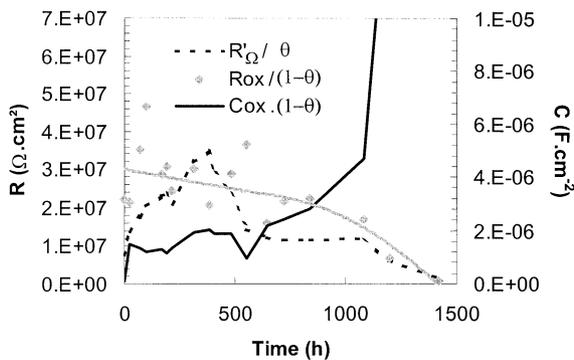

Fig. 8. Evolution of the parameters obtained from the fitting of the spectra obtained for plasma-coated Alclad 2024-T3 at different immersion times in 0.5 M NaCl solution.
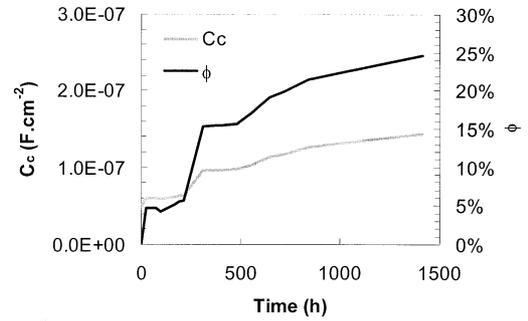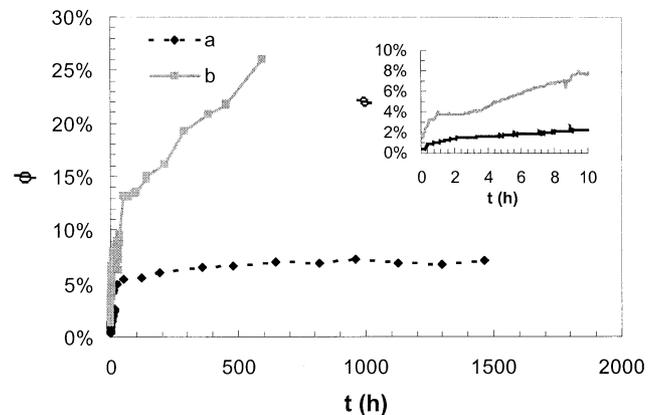

Fig. 10. Evolution of the water volume fraction at different immersion times in 0.5 M NaCl for plasma-coated samples showing: (a) high; and (b) low resistance to pitting corrosion.

changes are observed up to the end of the test. For the sample showing low resistance to pitting corrosion, only a small plateau is observed from 1 to 4 h of immersion, followed by a continuous rise in the ϕ values up to 26% by the 26th day of immersion, when the sample was removed from the testing solution with visible pits on its surface. As mentioned above, these last values of ϕ are not real, as they result from the calculation of a capacitance that is no longer a true coating capacitance, being affected by the onset of pitting corrosion.

From the analysis of Figs. 8 and 9, it becomes clear that the values of the coating capacitance or water volume fraction are more sensitive to the degradation of the coating than the values obtained by fitting to the equivalent circuit proposed in Fig. 1. The rise expected in the θC_{ox} values with the beginning of pitting is only noticed after 1100 h of immersion, whereas the sudden rise in C_c and ϕ values indicate a deterioration of the coating performance much earlier, at the fourth hour of immersion. In fact, the onset of pitting may be considered as a result of previous delamination or blistering in the coated system. On the opposite side, a specimen where the water uptake reaches a value of 4–5%, typical of other organic coatings, with no further rise on the values of ϕ, will be protected by the coating layer and no pitting corrosion is found up to the end of the immersion test.

4. Conclusions

Plasma coatings obtained by the plasma deposition of HMDSO improve the corrosion resistance of the Alclad 2024-T3 alloy. These coatings provide improved durability compared to the uncoated material.

The equivalent circuits proposed for the immersion behaviour of uncoated and plasma-coated material are consistent with the EIS spectra, allowing for the determination of the parameters relative to natural aluminium oxide, coating layer and pitting.

The calculation of water uptake of the plasma coating leads to a steady value of the water volume fraction of 4–5% in specimens that exhibit a good resistance to corrosion during the immersion tests. For samples that suffer pitting breakdown during the 60 days immersion period, a steep rise in the values of ϕ is detected since the early times of immersion, indicating that a delamination process may be taking place, which leads to the failure by pitting.

The evaluation of the corrosion performance of these coated materials by means of their water uptake behaviour may be useful, as the parameter ϕ seems to be much more sensitive to the changes in the system due to delamination than the values obtained from the fitting of EIS data to an equivalent circuit.

References

[1] J. Schwarz, M. Schmidt, A. Ohl, Surf. Coat. Tech. 98 (1998) 859.

[2] Y. Iriyama, T. Ihara, M. Kiboku, Thin Solid Films 287 (1996) 169.

[3] C.M. Reddy, Q.S. Yu, C.E. Moffitt, D.M. Wieliczka, R. Johnson, J.E. Deffeyes, H.K. Yasuda, Corrosion 56 (2000) 819.

[4] Q.S. Yu, C.M. Reddy, C.E. Moffitt, D.M. Wieliczka, R. Johnson, J.E. Deffeyes, H.K. Yasuda, Corrosion 56 (2000) 887.

[5] R.H. Turner, I. Segall, F.J. Boerio, G.D. Davis, J. Adhes. 62 (1997) 1.

[6] J.C.S. Fernandes, M.G.S. Ferreira, D.B. Haddow, A. Goruppa, R. Short, ATB Metallurgie XXXX (3–4) (2000); XXXXI (1–2) (2001) 192.

[7] F. Mansfeld, J. Appl. Electrochem. 25 (1995) 187.

[8] F. Deflorian, L. Fedrizzi, P.L. Bonora, Corros. Sci. 38 (1996) 1697.

[9] D.M. Brasher, A.H. Kingsbury, J. Appl. Chem. 4 (1954) 62.

[10] J.C.S. Fernandes, M.G.S. Ferreira, D.B. Haddow, A. Goruppa, R. Short, D.G. Dixon, Plasma-polymerised coatings used as pretreatment for aluminium alloys, submitted to publication in Surf. Coat. Tech. 154 (2002) 8.

[11] K. Jüttner, Electrochim. Acta 35 (1990) 1501.

[12] G.R.T. Schueller, S.R. Taylor, E.E. Hajcsar, J. Electrochem. Soc. 139 (1992) 2799.

[13] M.W. Kendig, F. Mansfeld, Proc. Fall Meeting Electrochem. Soc. 82-2 (1982) 105.

[14] R. Oltra, M. Keddam, Corros. Sci. 28 (1988) 1.

[15] F. Mansfeld, S. Lin, S. Kim, H. Shih, Mater. Sci. Forum 44–45 (1989) 83.

[16] F. Mansfeld, Electrochim. Acta 35 (1990) 1533.

[17] F. Mansfeld, H. Shih, H. Greene, C.H. Tsai, Analysis of EIS data for common corrosion processes, in: J.R. Scully, D.C. Silverman, M.W. Kendig (Eds.), Electrochemical Impedance—Analysis and Interpretation, ASTM, Philadelphia 1993, p. 37.

[18] F. Mansfeld, Analysis and interpretation of EIS data for metals and alloys, Schlumberger Technical Report 26, Schlumberger Technologies, Farnborough, 1993.

[19] J.C.S. Fernandes, PhD Thesis, Instituto Superior Tecnico, Lisbon, Portugal, 1997.

[20] G.W. Walter, Corros. Sci. 32 (1991) 1085.

[21] C.G. Oliveira, M.G.S. Ferreira, A new approach for ranking intact painting systems using EIS (Part I), submitted to Corros. Sci.